UNIVERSITY OF LEEDS

This is a repository copy of *Modelling built-up expansion and densification with multinomial logistic regression, cellular automata and genetic algorithm*.

White Rose Research Online URL for this paper:
http://eprints.whiterose.ac.uk/122357/

Version: Accepted Version

Article:

White Rose
university consortium
Universities of Leeds, Sheffield & York

eprints@whiterose.ac.uk
https://eprints.whiterose.ac.uk/

Modelling built-up expansion and densification with multinomial

logistic regression, cellular automata and genetic algorithm

Ahmed MUSTAFA (Corresponding Author)
LEMA, Urban and Environmental Engineering department, Liège University, Belgium.
Department of Computer Science, Purdue University, USA.

Permanent address:
Liège University, Allée de la Découverte 9, Quartier Polytech 1, 4000 Liège, Belgium
Tel.: +32 43 66 9394
Email: a.mustafa@ulg.ac.be
Present address:
Purdue University, Department of Computer Science, 305 N University St, West Lafayette, 47907 IN, USA.
Tel.: +1 765 250 1765.
Email: a-mustafa@purdue.edu

Alison HEPPENSTALL
School of Geography, University of Leeds, UK
E-mail: a.j.heppenstall@leeds.ac.uk

Hichem OMRANI
Urban Development and Mobility Department, LISER, Luxembourg
E-mail: hichem.omrani@liser.lu

Ismaïl SAADI
LEMA, Urban and Environmental Engineering department, Liège University, Belgium.
E-mail: ismail.saadi@ulg.ac.be

Mario COOLS
LEMA, Urban and Environmental Engineering department, Liège University, Belgium.
Email: mario.cools@ulg.ac.be

Jacques TELLER
LEMA, Urban and Environmental Engineering department, Liège University, Belgium.
Email: jacques.teller@ulg.ac.be

Modelling built-up expansion and densification with multinomial

logistic regression, cellular automata and genetic algorithm

Abstract: This paper presents a model to simulate built-up expansion and densification based on a combination of a non-ordered multinomial logistic regression (MLR) and cellular automata (CA). The probability for built-up development is assessed based on (i) a set of built-up development causative factors and (ii) the land-use of neighboring cells. The model considers four built-up classes: non built-up, low-density, medium-density and high-density built-up. Unlike the most commonly used built-up/urban models which simulate built-up expansion, our approach considers expansion and the potential for densification within already built-up areas when their present density allows it. The model is built, calibrated, and validated for Wallonia region (Belgium) using cadastral data. Three 100×100m raster-based built-up maps for 1990, 2000, and 2010 are developed to define one calibration interval (1990-2000) and one validation interval (2000-2010). The causative factors are calibrated using MLR whereas the CA neighboring effects are calibrated based on a multi-objective genetic algorithm. The calibrated model is applied to simulate the built-up pattern in 2010. The simulated map in 2010 is used to evaluate the model's performance against the actual 2010 map by means of fuzzy set theory. According to the findings, land-use policy, slope, and distance to roads are the most important determinants of the expansion process. The densification process is mainly driven by zoning, slope, distance to different roads and richness index. The results also show that the densification generally occurs where there are dense neighbors whereas areas with lower densities retain their densities over time.

Keywords: Built-up density; cellular automata; multinomial logistic regression; multi-objective genetic algorithm

1. Introduction

Built-up development is the most typical form of land-use change. Without policy

interventions, built-up developments may cause destructive impacts on the environment, on

natural resources and on human health (Zhang et al., 2011). Consequently, modelling built-up

development is attracting attention of scientists, urban planners and politicians alike. Most built-

up/urban models (e.g. Han and Jia, 2016; Liao et al., 2014; Liu et al., 2014; Puertas et al., 2014;

Vermeiren et al., 2012) are raster-based with a coarse cell space ranging from 30×30m to

300×300m. Whilst many authors advocate a larger grid cell for land-use modelling, for example

100×100m (e.g. Jiang et al., 2007; Munshi et al., 2014; Poelmans and Van Rompaey, 2010),

land-use cells with these dimensions usually comprise a mix of different land-uses (Omrani et

al., 2015). For example, a cell classified as built-up land may be occupied by 80% built-up

surface and 20% arable surface. With increases in the spatial resolution of data, researchers have

begun to use grid cells as small as 10×10m, such as Berberoğlu et al. (2016) model for Adana

city (Turkey). However, the drawback to using such a fine resolution is that it requires intensive

computational resources to model larger study areas such as regions where 100×100m cell

dimensions are commonly used (e.g. Omrani et al., 2015; Poelmans and Van Rompaey, 2010).

One solution to address the trade-off between coarse regular cell spaces and heterogeneity is

examining several built-up densities instead of a binary classification (i.e. non built-up/built-up).

Although built-up densification processes, transitions from low-density to high-density, is

critically important for policy makers who are concerned with restricting sprawl (Nabielek,

2012; Tachieva, 2010), the literature on urban/built-up expansion models highlights that many of

the models focus only on expansion process (e.g. Poelmans and Van Rompaey, 2009; Wang et

al., 2013). However, there are a limited number of studies that consider the expansion of several urban densities and/or densification in a variety of ways. Mustafa et al. (2015), Robinson et al. (2012), Sunde et al. (2014), Xian and Crane (2005), Yang (2010) and Zhang et al. (2011) model the expansion of different urban/built-up densities. Crols et al. (2015), Loibl and Toetzer (2003) and White et al. (2015, 2012) model the processes of urban expansion as well as of densification. They define densification as an increase in population and/or several economic sectors density.

One of the most popular techniques of existing urban/built-up expansion models which are employed to analyze and/or predict the built-up pattern is cellular automata (CA) (e.g. Berberoğlu et al., 2016; Feng et al., 2011; Han et al., 2009; Tian et al., 2016; Wang et al., 2013). CA is a dynamic discrete space and time bottom-up modelling approach. CA is widely used in urbanization modeling due to its simplicity, transparency and powerful capacities for dynamic spatial simulation (Clarke and Gaydos, 1998). Aburas et al. (2016) and Santé et al. (2010) reviewed CA urbanization models concluding that the CA modelling approach is one of the most appropriate techniques for simulating urban/built-up patterns. However, key challenges in CA are calibrating the transition rules of built-up development probability as a function of (i) a series of causative factors (driving forces) and (ii) spatial (neighborhood) characteristics. Early methods for CA calibration are based on trial and error (e.g. White and Engelen, 1997) and/or a visual test, to determine the model's parameters (e.g. Clarke et al., 1997; Ward et al., 2000). Recently, a variety of automated methods based on statistics (e.g. García et al., 2013), machine learning (e.g. Rienow and Goetzke, 2015), artificial neural networks (e.g. Berberoğlu et al., 2016) and search algorithms for optimization such as genetic algorithms (e.g. Al-Ahmadi et al., 2009) and particle swarm optimization (e.g. Feng et al., 2011) have begun to be widely employed.

46   Validation of CA models is another challenge. A common validation method is based on

47 pixel-by-pixel location agreement (Poelmans and Van Rompaey, 2009). This approach cannot

48 discriminate between "near-miss" and "far-miss" errors which limits its ability to detect spatial

49 patterns (Mustafa et al., 2014). Another approach is based on spatial metrics (Roy Chowdhury

50 and Maithani, 2014). Spatial metrics can be potentially misleading, for example, two areas with

51 distinctly different infrastructures may show the same spatial index (White and Engelen, 2000).

52 A third method is based on a fuzzy set theory. Fuzzy map comparison provides a method of

53 dealing and comparing maps containing a complex mixture of spatial information (Ahmed et al.,

54 2013). It takes into account local variations meaning that matches found at shorter distances are

55 given a higher agreement. It measures the similarity of a cell in a value between 0 (fully-distinct)

56 and 1 (fully-identical). Thus, it can easily distinguish areas of minor errors from areas of major

57 errors. Van Vliet et al., 2016 present a comprehensive survey of calibration and validation

58 practices in land use change modeling.

59   This study contributes to research efforts that model built-up expansion and densification

60 processes. We model the built-up expansion (non built-up to one of built-up density classes) and

61 densification (lower built-up densities to higher ones). The model is based on a hybrid approach

62 which integrates logistic regression and CA modelling approaches. The model is applied to

63 Wallonia (Belgium). Belgian cadastral data (CAD) are used to generate three built-up maps for

64 the years 1990, 2000 and 2010. These maps represent four built-up classes: non built-up (class-

65 0), low-density (class-1), medium-density (class-2) and high-density (class-3). Three maps can

66 define one calibration interval (1990-2000) and one validation interval (2000-2010). The model

67 considers a set of static causative factors related to accessibility, geo-physical features, policies

68 and socio-economic factors. Another important factor is neighborhood interactions because of

the fact that urbanization can be regarded as a self-organizing system (Poelmans and Van

Rompaey, 2010).

The model's parameters are calibrated based on a logistic regression model and genetic

algorithm. The logistic regression is employed to set the parameter of 12 built-up development

causative factors: elevation, slope, zoning status, employment rate, richness index and Euclidian

distances to highways, main roads, secondary roads, local roads, railway stations, large-sized and

medium-sized Belgian cities. The richness index is calculated as the average income per capita

for each municipality divided by the average income per capita in Belgium. The built-up

causative factors are selected according to a literature survey of common factors involved in

urban/built-up expansion models (e.g. Achmad et al., 2015; Cammerer et al., 2013; Dubovyk et

al., 2011; Li et al., 2013; Poelmans and Van Rompaey, 2010; Verburg et al., 2004) as well as the

finding of previous studies conducted for Wallonia (Beckers et al., 2013; Mustafa et al., 2015).

The dependent variable for the logistic regression model represents the changes from class-0 to

class-1, class-2 or class-3, the changes from class-1 to class-2 and the changes from class-2 to

class-3.

As the dependent variable is a multi-level, i.e. with more than two possible outcomes, we

should consider a non-binary logistic regression. The most common logistic regression types that

handle multiple levels of an outcome are ordered logistic regression and multinomial logistic

regression. Ordered logistic regression assumes that the levels of dependent status have a natural

ordering (i.e. low to high). This is known as the proportional odds model or parallel regression

assumption (Kim, 2003). To evaluate this assumption, the test of the proportional odds

assumption is performed. The null hypothesis of the test is that the relationship, i.e.

coefficients, between each pair of dependent levels is the same. The significance of Chi-Square

92   statistic of the proportional odds test is < 0.001. Given the assumption of having a natural

93   ordering in the dependent variable is violated, thus a non-ordered multinomial logistic regression

94   model (MLR) is adopted for this study.

95   A multi-objective genetic algorithm (MGA) is employed to calibrate the neighborhood

96   interactions on a dynamic basis. García et al., (2013) reported that the GA is one of the most

97   robust heuristic automated methods to solve optimization problems. A number of studies have

98   used GA to calibrate CA models (e.g. Al-Ahmadi et al., 2009; García et al., 2013; Shan et al.,

99   2008). The MGA objective function is the maximization of allocation accuracy rates for all built-

100   up classes. The accuracy rate function is defined as a fuzzy membership function of exponential

101   decay with a halving distance of two cells and a neighborhood window of four cells. The

102   accuracy rate function is also employed to validate the model.

103   **2. Materials**

104   **2.1 Study area**

105   The model is applied to Wallonia region, the southern part of Belgium. Wallonia occupies an

106   area of 16,844 km² and administratively consists of five provinces: Hainaut, Liège, Luxembourg,

107   Namur, and Walloon Brabant. The total population in 2010 was 3,498,384 inhabitants,

108   corresponding to one third of the Belgium population (Belgian Federal Government, 2013). The

109   population is mainly concentrated on the northern areas, following the 19th century industrial

110   axis, running from east (Liège) to west (Mons) (Thomas et al., 2008). The rest of the territory is

111   less densely inhabited. Consequently, several densities can be easily detected in the region and

112   thus we can examine the transitions between different densities. The built-up development is

mainly characterized by low, slow rates, which makes the calibration of the model more difficult

because there is less information on the built-up process (García et al., 2012). The expansion

rates were 1.18% and 0.79% from 1990 to 2000 and from 2000 to 2010, whereas the
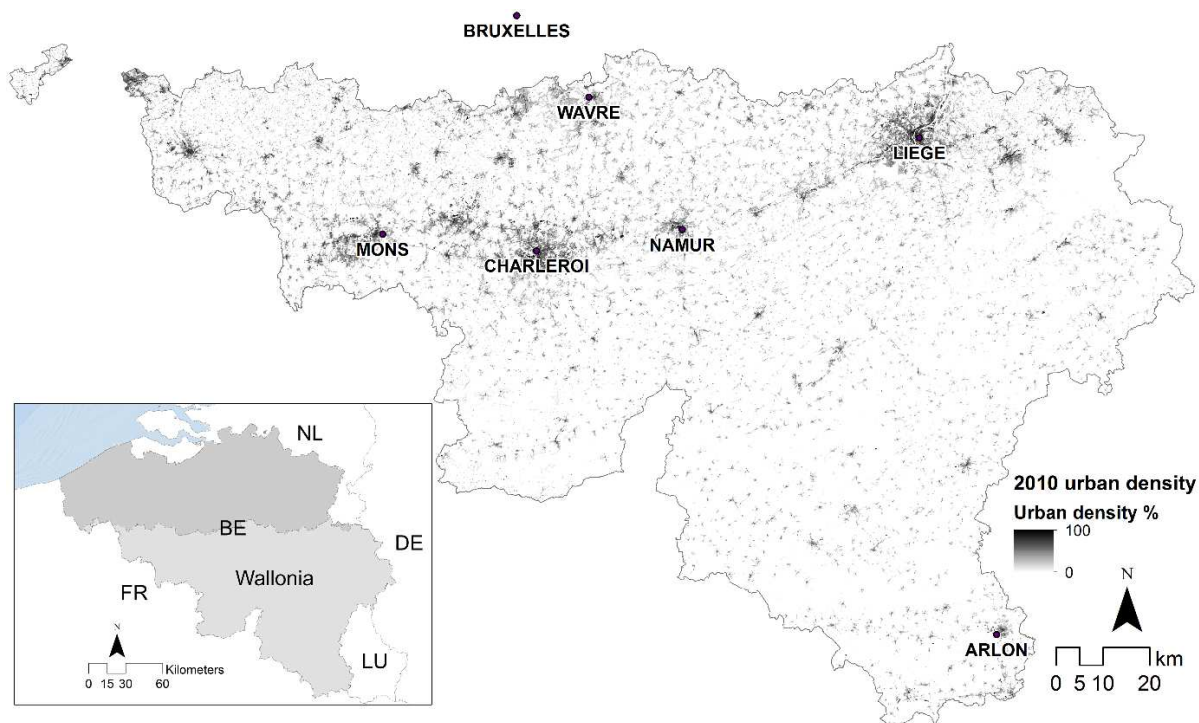
densification rates were 12.18% and 9% respectively.

Figure 1: Study area.

Table 1 gives the actual built-up transitions over the modeled period for four density classes

(Table 2). As in Xian and Crane (2005), the table suggests that the predominant built-up

processes have been the development of low-density and medium-density areas. The majority of

the new developments have a form of built-up sprawl. This development process had resulted in

a highly fragmented built-up pattern. Table 1 indicates that the transitions from class-1 to class-3

over the study period are marginal. Thus, the densification is considered as the transitions from

class-1 to class-2 and from class-2 to class-3, whereas the expansion are the transitions from

class-0 to classes 1, 2 and 3.

Table 1. Class (column) to class (row) changes (% of the reference class).

1990-2000	Class-0	Class-1	Class-2	Class-3
Class-0	1422166 (98.82%)	0	0	0
Class-1	10841 (0.75%)	85142 (89.25%)	0	0
Class-2	5153 (0.36%)	10102 (10.59%)	128929 (98.57%)	0
Class-3	1016 (0.07%)	151 (0.16%)	1872 (1.43%)	25284
2000-2010	Class-0	Class-1	Class-2	Class-3
Class-0	1410959 (99.21%)	0	0	0
Class-1	7120 (0.50%)	88341 (92.04%)	0	0
Class-2	3450 (0.24%)	7535 (7.85%)	142687 (98.96%)	0
Class-3	637 (0.04%)	107 (0.11%)	1497 (1.04%)	28323

2.2. Datasets

The built-up maps for 1990, 2000 and 2010 are generated based on the Belgian cadastral

database (CAD) in a shapefile format. CAD is provided by the Land Registry Administration of

Belgium. The information contained includes the construction date for each building. CAD

vector data were rasterized at a cell size of 2×2m. The rasterized cells were then aggregated to a

100×100m raster-grid. The density values were calculated for the aggregated cells (100×100m)

by counting the smallest cells (2×2m). All aggregated cells with a density values less than 25

were considered as non built-up cells. The threshold of 25 (representing a building of 100m²)

corresponds to an average-sized residential building in Belgium (Tannier and Thomas, 2013).

All 100×100m cells have a density index ranging between 0 and 2500. The density index is

then used to set four classes: non-built-up (class-0), low-density (class-1), medium-density

(class-2) and high-density (class-3). A geometrical interval classification method is used to set

the density ranges that define the different classes. This classification method works very well on

138 continuous data (Arlinghaus and Kerski, 2013). The resulting density ranges are listed in Table

139 2.

Table 2. Built-up density classes range in number of 2×2 cells (% of 100x100 cell area).

Class	Minimum	Maximum
Class-0 (non built-up)	0	24 (1)
Class-1 (low-density)	25	102 (4.1)
Class-2 (medium-density)	103	499 (20)
Class-3 (high-density)	500	2500 (100)

140 The built-up development causative factors were operationalized to be included in the MLR.

141 Table 3 gives the selected factors for this study. The socio-economic data (employment rate and

142 richness index) come from the Belgian statistics, published by The Walloon Institute for

143 Evaluation, Prospective and Statistics. The elevation data are derived from the Belgian National

144 Geographic Institute. The distance to the different road categories are derived from a vector

145 dataset made available by Navteq Company. The Navteq dataset identifies the following

146 categories of roads: Road1 (highways), Road2 (main roads), Road3 (secondary roads), Road4

147 (local roads). The location of railway stations are provided by Walphot SA Company. This study

148 considers distance to large-sized cities (population greater than 90,000) and medium-sized

149 Belgian cities (population between 20,000 and 90,000). The distance-based factors are based on

150 the Euclidean distance to selected features. Euclidean distance is widely used in land-use change

151 models (Poelmans and Van Rompaey, 2009; Roy Chowdhury and Maithani, 2014). Zoning areas

152 were obtained from the regional zoning plan, commonly named as PDS (plan de secteur) in

153 Wallonia. A zoning map was developed by discriminating between the zones where built-up

154 development is legally permitted and those where it is not.

155

Table 3. List of selected built-up causative factors.

Factor	Name	Type	Unit
X_1	Elevation (DEM)	Continuous	Meter
X_2	Slope	Continuous	Percent rise
X_3	Dist. to Road1	Continuous	Meter
X_4	Dist. to Road2	Continuous	Meter
X_5	Dist. to Road3	Continuous	Meter
X_6	Dist. to Road4	Continuous	Meter
X_7	Dist. to railway stations	Continuous	Meter
X_8	Dist. to large-sized cities	Continuous	Meter
X_9	Dist. to med-sized cities	Continuous	Meter
X_{10}	Employment rate	Continuous	Percent
X_{11}	Richness index	Continuous	Percent
X_{12}	Zoning	Categorical	Binary (0 non built-up, 1 built-up)

3. Methodology

In this study, an integrated MLR and CA model is developed. The model considers two built-up processes: (1) built-up expansion (transitions from non-built-up to built-up) and (2) built-up densification (transitions from lower built-up densities to higher ones). This section discusses the main characteristics of the model. The quantity of change during calibration (1990-2000) and validation (2000-2010) phases was constrained to the actual quantity of new built-up lands, table 1, divided evenly by 10 (the number of years).

3.1 The transition rules

The quantity of change is spatially allocated based on a transition rule which has two components. The first component concerned the main built-up causative factors as determined using MLR (section 3.1.1). The second component dealt with the neighborhood characteristics (section 3.1.2). The transition potentials P for a cell ij changing its state from non-built-up to one

of the built-up densities or low density built-up to a higher one at specific time-step is calculated

as follows:

$$P_{ij} = \sqrt{(P_c)_{ij} \times (P_n)_{ij}^{\sigma}} \tag{1}$$

where $(P_c)_{ij}$ is the built-up probability based on built-up causative factors, $(P_n)_{ij}^{\sigma}$ is the

neighborhood effect on the cell ij and σ expresses the relative importance of the neighborhood

effect. Figure 2 demonstrates an example of how the final transition potential P matrix is

calculated.

0.31	0.97	0.88
0.42	0.92	0.76
0.02	0.94	0.52

$\odot$

14.1^2	2^2	6.2^2
16.2^2	2.8^2	7.1^2
7.8^2	4.2^2	8.6^2

$\blacktriangleright$

7.9	2	5.8
10.5	2.7	6.2
1.1	4.1	6.2

Figure 2: An example of built-up transition potentials matrix (right) which equals the square root of pairwise multiplication of P_c (left) and P_n (middle) matrices. The relative importance (σ) of P_n is assumed to be 2.

The model selects the top-scoring cells from the built-up transition potentials matrix for each

density class and changes their state to the appropriate class until meeting the required quantity.

The transition potential matrices are calibrated for 1990-2000. The calibration results are then

used to simulate 2000-2010 built-up pattern. The simulated map of 2010 is compared against the

actual 2010 map to validate the model allocation ability (section 3.2).

3.1.1. Built-up development causative factors calibration

The $(P_c)_{ij}$ can be determined through a set of factors described in Table 3 using the MLR. The

MLR is a model to discover the empirical relationships between a multi categories dependent

variable and several independent variables (built-up development causative factors). The model

performed for class-0 (dependent variable represents non-changes/changes from class-0 to class-

1 or class-2 or class-3), for class-1 (dependent variable represents non-changes/changes from class-1 to class-2) and for class-2 (dependent variable represents non-changes/changes from class-2 to class-3).

The general form of the MLR can be represented as:

$$\log(k_1) = \alpha_{k_1} + \beta_{k_1 1}X_1 + \beta_{k_1 2}X_2 + ... + \beta_{k_1 v}X_v$$
$$...$$
$$\log(k_n) = \alpha_{k_n} + \beta_{k_n 1}X_1 + \beta_{k_n 2}X_2 + ... + \beta_{k_n v}X_v$$

$$(2)$$

where $log(k_n)$ is the natural logarithm of class k_n versus the reference class k_0, X is a set of explanatory variables $(X_1, X_2,..., X_v)$, α_{k_n} is the intercept term for class k_n versus the reference class and β is the slopes for the classes (the coefficient vector). Thus, the probabilities of each class can be obtained using the following formula:

$$((P_c)_{ij}, Y = k_0) = \frac{1}{1 + \exp(\log(k_1)) + \exp(\log(k_2)) + ... + \exp(\log(k_n))}$$
$$((P_c)_{ij}, Y = k_1) = \frac{\exp(\log(k_1))}{1 + \exp(\log(k_1)) + \exp(\log(k_2)) + ... + \exp(\log(k_n))}$$
$$...$$
$$((P_c)_{ij}, Y = k_n) = \frac{\exp(\log(k_n))}{1 + \exp(\log(k_1)) + \exp(\log(k_2)) + ... + \exp(\log(k_n))}$$

$$(3)$$

where $((P_c)_{ij}, Y=k_n)$ is the probability of change from the reference class to class k_n occurring in cell ij. The MLR employs the maximum likelihood estimation method to achieve the best fit sets of coefficients for each X.

The MLR outcomes are a set of coefficients that define the relative contribution of each factor to the built-up process, as well as a set of maps of probability of built-up for each class that are generated by inserting the coefficients of the MLR model into Equation (3).

199 The goodness-of-fit of the MLR is evaluated using the relative operating characteristic (ROC)

200 method. The ROC is an excellent method to estimate the quality of a model that predicts the

201 occurrence of an event by comparing a probability map of that event occurring and a binary map

202 presenting the actual changes (Hu and Lo, 2007). A ROC value of 0.5 means a completely

203 random discrimination and 1 means a perfect one.

204 All the data layers were resampled to the same cell resolution of 100×100m. The *X-variables*

205 are measured in different units and therefore we standardized all continuous *X-variables*. If some

206 of *X-variables* relatively measure the same phenomena, then strong collinearities will cause the

207 erroneous estimation of the parameters. A multicollinearity test was examined in the initial stage

208 using variance inflation factors (VIF) to ensure that there are not two or more causative factors

209 measuring the same phenomena. (Montgomery and Runger, 2003) recommended that the VIF

210 values should not exceed 4.

211 The dependent variables may show spatial autocorrelation, which biases the results of the

212 regression analysis (Overmars et al., 2003). This issue can be addressed through a data sampling

213 approach (Cammerer et al., 2013; Poelmans and Van Rompaey, 2010; Rienow and Goetzke,

214 2015). A sample of 29300 cells was randomly selected. For each reference class, other existing

215 classes in 1990 are excluded from the sampling, e.g. expansion (class-0) sampling procedure

216 considers new transitions from class-0 to class-0, class-1, class-2 and class-3. The selection of

217 samples is based on 100 runs of the MLR with different random samples. The best sample set,

218 evaluated by ROC, is then selected.

3.1.2. Cell neighborhood calibration

Neighborhood interactions can also be calibrated in MLR model by including them as part of the explanatory variables (Hu and Lo, 2007; Verburg et al., 2004). However, because MLR models are not temporally explicit, they cannot reveal the path-dependent and self-organizing development which is typical for urban expansion (Poelmans and Van Rompaey, 2010; Wu, 2002). The most common approach to explicitly calibrate the neighborhood interactions on a dynamic basis is by using a cellular automata (CA) modelling approach.

In some studies (e.g. Chen et al., 2014; Poelmans and Van Rompaey, 2009; Wu, 2002) the neighborhood is defined as a square region, the Moore neighborhood, around the central cell with many square sizes from 3×3 to 11×11. Chen et al. (2014) and Poelmans and Van Rompaey (2009) analyzed several square sizes and concluded that the model run with the 3×3 neighborhood window produces a land-use pattern that most fits the actual pattern. These studies use a coarse cell resolutions. However, it might be different for finer cell resolutions. In this study, a 3×3 neighborhood window is used to consider neighborhood interactions. The $(P_n)_{ij}$ is calculated according to the method proposed by White and Engelen (2000):

$$\left(P_n\right)_{ij} = \sum_k \sum_x \sum_d w_{kxd} \cdot I_{kxd} \tag{4}$$

where w_{kxd} is the weighting parameter assigned to a cell with class k, which represents one of the built-up classes listed in table 2, at position x at distance zone d and I_{kxd} is 1 if a cell in distance d is occupied by class k or 0 otherwise.

Our objective is to define the CA parameters that achieve the best allocation accuracy rate for the expansion process (transitions from class-0 to class-1, class-2 and class-3 simultaneously)

239 and for the densification process (transitions from class-1 to class-2 and transitions from class-2

240 to class-3). In order to automatically calibrate the neighborhood weighting parameters, a multi-

241 objective genetic algorithm (MGA) is used for the expansion and a genetic algorithm (GA) is

242 used for the densification process. The genetic algorithm is a highly effective algorithm for

243 solving both constrained and unconstrained optimization problems that has been inspired by the

244 mechanisms of evolution and genetics (Al-Ahmadi et al., 2009; Holland, 1975). MGA attempts

245 to portray a trade-off among multiple, possibly conflicting objectives at once. In this paper,

246 MGA is a variant of a non-dominated sorting genetic algorithm II (NSGA-II) proposed by (Deb,

247 2001). NSGA-II favors individuals with an elitist strategy and individuals that can help increase

248 the diversity of the population (Yijie and Gongzhang, 2008). The output of the MGA is a set of

249 solutions that is also known as Pareto front optimized solutions, among which we can select the

250 most preferable solution. Pareto front is a set of feasible solutions that are non-dominated to each

251 other but are significantly better than the rest of solutions.

252 The MGA/GA initializes a random initial population in which many solutions participate in an

253 iteration (generation). It then uses stochastic operators to generate new generations and direct a

254 searching process based on a fitness function. Each individual in the population corresponds to a

255 chromosome made up of a set of genes, where each gene represents one parameter that requires

256 calibration. In each generation, every individual in the population is evaluated through a fitness

257 function. Once the initial population is generated and evaluated, the parents for the next

258 generation are selected by using a tournament procedure based on a relative fitness score. In this

259 paper, the tournament randomly selects two individuals, and the individual with the highest

260 fitness value becomes a parent. Each two parents are combined based on a crossover operator.

261 We proposed that the crossover operator generates two children that lie on the line representing

both parents and inherit at least 70% genes from the parent with the better fitness value. Once the new generation is obtained, each child is then perturbed in its vicinity by a mutation operator that adds a small random number to each gene.

This study tries to achieve a proper balance between exploration and exploitation ability of the MGA/GA. Exploration enables the MGA/GA to explore a broader search space, while exploitation enables MGA/GA to focus on one direction which is an optimal solution or close to it (Hansheng and Lishan, 1999). The mutation operator is used to provide exploration ability whereas the crossover operator is used to lead the population to the global optimal solution so far. In our case, the mutation operator selects a random number from a Gaussian distribution with a center of zero and a standard deviation of 2 at the first generation. This standard deviation is shrunk to 0 linearly as the last generation is reached. Consequently, the MGA/GA explores much more search space at the beginning of the optimization process and ensures the convergence of the population towards the global optimal solution by the end of the process.

MGA/GA is initialized with a random population. Stochastic operators are applied to this population and a large number of generations evolved to obtain a favorable solution. Each individual solution takes about 19 seconds in case of MGA and 8 seconds in case of GA to be evaluated using a good PC (Intel Core i7-4700 CPU @ 2.4GHz) implying that large population and generation numbers require considerable time to be processed. To minimize the computing time, we implement a two phase MGA/GA. First, the MGA/GA starts with a low number of population and generations. Second, the outcome of the first run is used to set the initial population, initial range and number of generations. In addition, the first run is used to determine values for the crossover and mutation operators. Based on this, a set of 500 generations (300 for

expansion, 100 for densification of class-1 and 100 for densification of class-2) with 500

individuals for each generation are used for the final MGA/GA.

The objective function for the genetic algorithms for the calibration is based on a fuzzy

membership function, as discussed further below. The parameter values that maximize the

objective function will be selected as the best calibration outcome.

3.2. Validation

The ability of the model to locate transitions from non-built-up to one of built-up densities and

lower densities to higher densities is validated by comparing the simulated map of 2010 with the

actual map of 2010. The comparison considers only new built-up transitions between 2000 and

2010. The fuzziness index of a cell location depends on the cell itself and the cells in its

neighborhood. There is no universally agreed extent to which the neighboring cells influence the

fuzzy representation and a type of decay function among land-use modelers. Although it may be

advantageous to experiment with different neighboring sizes and decay functions to define the

best alternative, this experiment is beyond the scope of this paper as it would require too much

space to adequately discuss such analyses. However, a number of authors proposed an

exponential decay function with a halving distance of two cells and a neighborhood with a four-

cell radius to evaluate (Ahmed et al., 2013; Hagen, 2003; Loibl et al., 2007). Likewise, the

average fuzziness index used in this paper is an exponential decay with a halving distance of two

cells and a neighborhood with a four-cell neighbor extent and calculated as follows:

$$A_k = \frac{\sum\limits_{x_k \in X_{k,sim}} \left| I_{x_k 0} \cdot \left(1/2\right)^{0/2}, I_{x_k 1} \cdot \left(1/2\right)^{1/2}, \ldots\ldots, I_{x_k d} \cdot \left(1/2\right)^{d/2} \right|_{max}}{X_{k,actul}} \qquad (5)$$

303   where A_k ($0 \leq A \geq 1$) is the average fuzziness index for class k, $I_{x_k d}$ is 1 if cell x_k in the simulated

304   map in a neighborhood at zone d ($0 \leq d \geq 4$) is identical to one cell in neighborhood at zone d in

305   the actual map otherwise is 0, $X_{k,sim}$ is the total number of changed cells of class k in the

306   simulated map and $X_{k,actul}$ is the total number of changed cell of class k in the actual map. The

307   fuzziness index is also employed as the objective function for MGA/GA.

4. Results and discussion

309   In this section, the built-up pattern resulted from classification of CAD data, the calibration

310   results and the validation of the model are discussed. In general, the built-up pattern visible in

311   Wallonia resembles the classical built-up pattern from across a wide range of regions worldwide

312   (Kumar et al., 2012). A high level of built-up density was found in the major built-up cores

313   surrounded by medium-density built-up areas. A large majority of low-density lands are likely to

314   be found in scattered rural areas and remote locations. Figure 3 illustrates different densities for

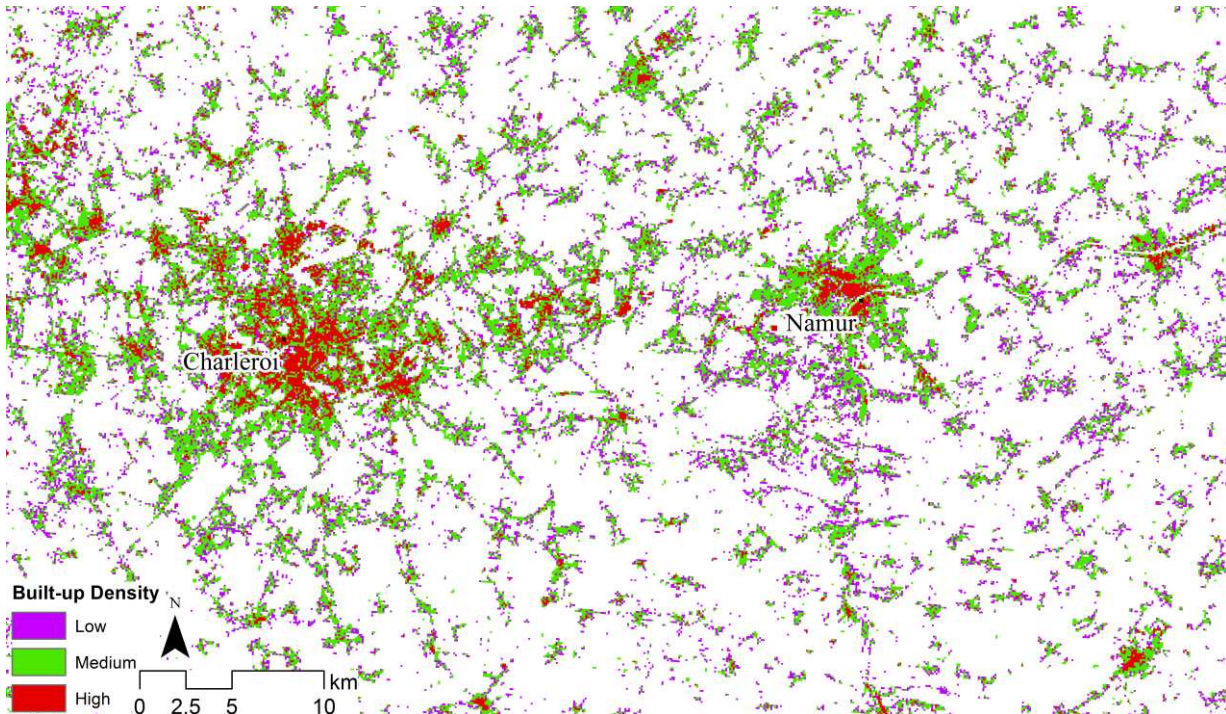315   Charleroi and Namur metropolitan areas as an example.

Figure 3: Built-up classes of 2010 for Charleroi and Namur metropolitan areas.

316   Variance inflation factors test, with values of less than 1.33, shows no problems with

317   multicollinearity suggesting that all causative factors can be incorporated in the MLR model. The

318   MLR parameter sets calibrated in the 1990–2000 are shown in Figure 4. According to the results,

319   the major causative factor of the expansion process is the zoning status and that is in-line with

320   Poelmans and Van Rompaey (2010). Zoning impact shows a steady upward trend along with

321   density. High-density developments are located in areas where the legally-binding plan allows

322   such developments, to avoid any possible administrative and financial risks. On the other hand,

323   built-up developments in areas adjacent to urban cores (class-2) like suburbs do not strictly

324   follow policies. The impact of policy on low-density developments is low compared to other

325   classes. This class can be considered as remote built-up areas, consisting in scattered buildings,

326   which can sometimes deviate from zoning plans. The magnitude of the zoning status influence

327 on the densification process is remarkably low compared to the expansion process. The fact that

328 the densification process is done within existing built-up areas, merely means that the zoning

329 plan does not have a strong effect on the densification processes. As in Poelmans and Van

330 Rompaey (2010) slope shows a negative effect on the development of built-up areas. Distance to

331 roads shows a negative effect on the built-up developments so that built-up transitions generally

332 occur close to roads as reported in Cammerer et al., (2013) and Poelmans and Van Rompaey

333 (2010). Distance to railway stations is statistically significant for the expansion of high-density

334 built-up suggesting that parcels nearby train stations are attractive for new dense developments.

335 Although the richness index is insignificant, as in Hu and Lo (2007), except for all medium-

336 density transitions, it implies that the medium-density developments are linked closely to the

337 income distribution. Medium-density can generally represent urban sprawl and suburbanization

338 which replace non-built-up lands with single-family houses on large lots. The richness index has

339 a positive impact on transition from non-built-up and low-density to medium-density implying

340 that affluent and middle-class people settle in medium-density built-up areas. In contrast, the

341 richness index has a strong negative impact on the transition from medium-density to high-

342 density so that most such transitions can be found in somewhat poor neighborhoods. Distance to

343 cities especially the medium-sized cities indicates a moderate negative impact on built-up

344 expansion processes and densification of low-density areas. That is in-line with Poelmans and

345 Van Rompaey (2010) who reported that urban development tends to occur near to the cities. As

346 in Hu and Lo (2007) and Poelmans and Van Rompaey (2010), employment rate has insignificant

347 impact on the expansion of most built-up densities and the densification process.
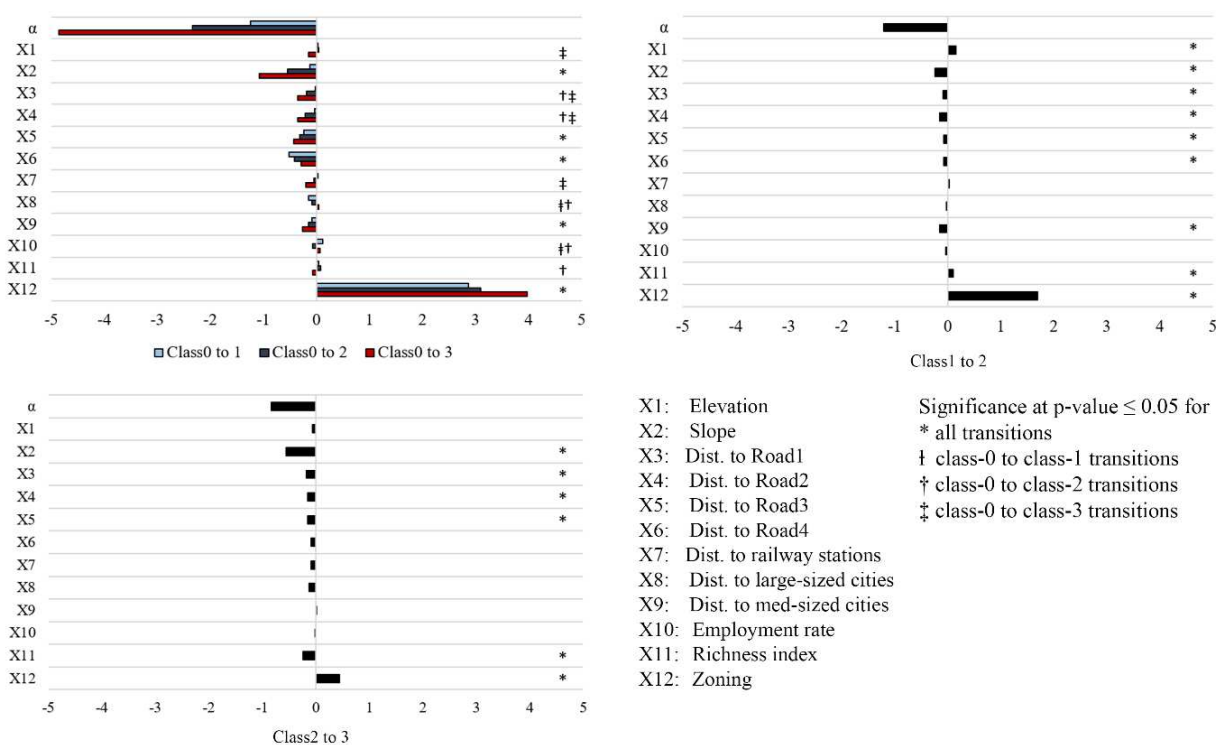
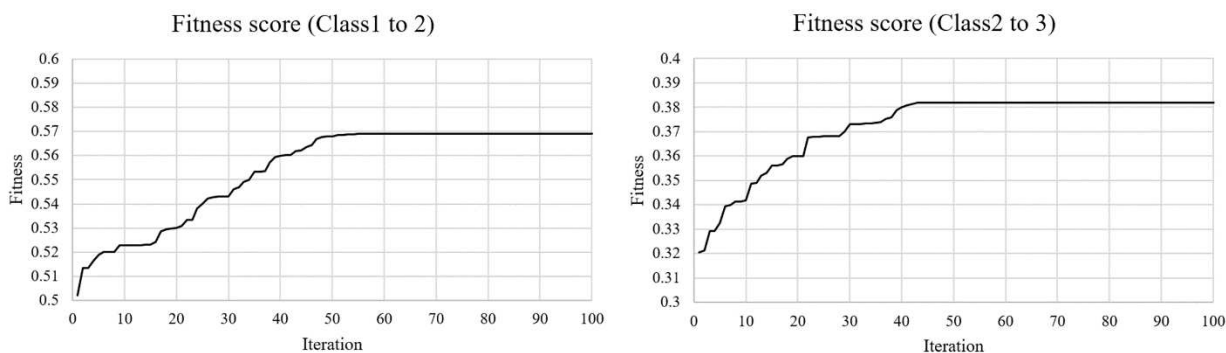**Figure 4:** The MLR parameters coefficients for 1990-2000.

Figure 5: The convergence of the fitness score during the GA optimization.

348   The GA optimization module for the densification of class-1 and class-2 began to converge

349   when reaching iteration 56 and 50 respectively (Figure 5). After 228 iterations, average

350   change in the spread of Pareto solutions for MGA was less than 0.00001. The MGA/GA

351   optimal weighting values that define neighborhood interactions are given in Figure 6 (a, b and c).

The calibration shows that the likelihood of low-density expansion is highly increased by increasing the number of existing low-density and medium-density lands and decreasing the number of high-density lands in the immediate neighborhood of the cell. The probability of medium-density expansion is increased with increasing number of all land-uses, especially medium-density cells. This study finds a positive relationship between expansion of high-density and the number of existing high-density cells in the neighborhood of the cell. In contrast, the expansion of high-density lands is negatively impacted by increasing the number of non built-up, low and medium-density lands. The probability of low to medium-density built-up transitions is positively linked with the existing non built-up, low and medium-density built-up neighbors and negatively linked with high-density neighbors, whereas the densification of medium-density areas is negatively related to the increasing number of non built-up and low-density cells and positively related to the increasing the number of high-density cells in the neighborhood of the cell. Together, these findings suggest that existing residents of low and medium-density areas tend to protest dense developments near their home, whereas most new densified areas are located within or close to already high-density neighbors. This causes a highly fragmented and low-density built-up landscape. One of the main factors leading to this situation is the spatial planning policy (Dieleman and Wegener, 2004; Poelmans and Van Rompaey, 2009).

The ROC values of the MLR outcomes are 0.81, 0.85, 0.94, 0.73 and 0.72 for class-0 to class-1, class-0 to class-2, class-0 to class-3, class-1 to class-2 and class-2 to class-3 respectively. ROC values higher than 0.70 are considered as a reasonable fit and the estimates can be used in further analyses (Cammerer et al., 2013; Jr and Lemeshow, 2004).

The calibration and validation of allocation accuracy rates are given in figure 6 (d). The relative importance of the neighborhood effect (σ) parameter is calibrated using MGA. The

MGA of σ converges when reaching iteration 35 for expansion process, 27 and 24 respectively for densification of class-1 and class-2. The value of parameter σ shows neutral effect, i.e. equals 1, on the expansion of class-2, class-3 and the densification of class-2. For the expansion and densification of low-density class the values of σ are 1.97 and 0.53 respectively.

The calibration accuracy rates are larger than the validation rate. The possible source of this variation is potentially due to the uncertainty associated with the future values of modeling parameters. Most CA models (e.g. Al-Ahmadi et al., 2009; García et al., 2013) introduced a stochastic disturbance term to represent unknown errors and uncertainty. The extension of this study necessitates a more comprehensive framework that explicitly quantifies and models uncertainty related to future values of the model's parameters.
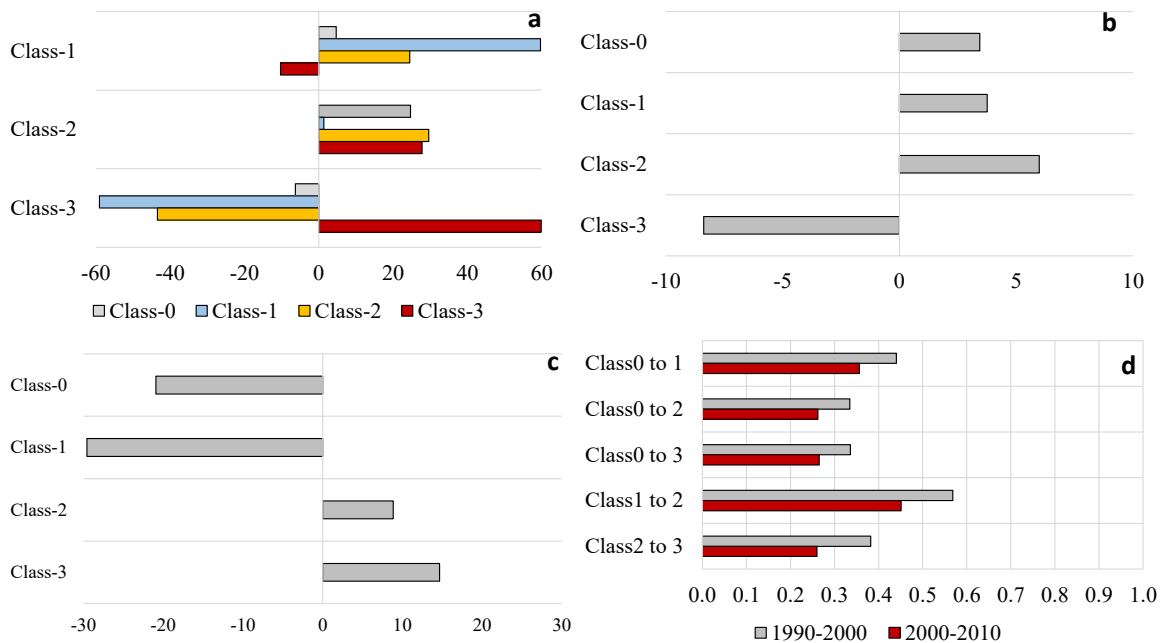

Figure 6: Weighting values that define neighborhood parameters values for (a) transitions from class-0 to class-1, class-2 and class-3, (b) transitions from class-1 to class-2 and (c) transitions from class-2 to class-3. (d) The average fuzzy similarity rates for calibration and validation.
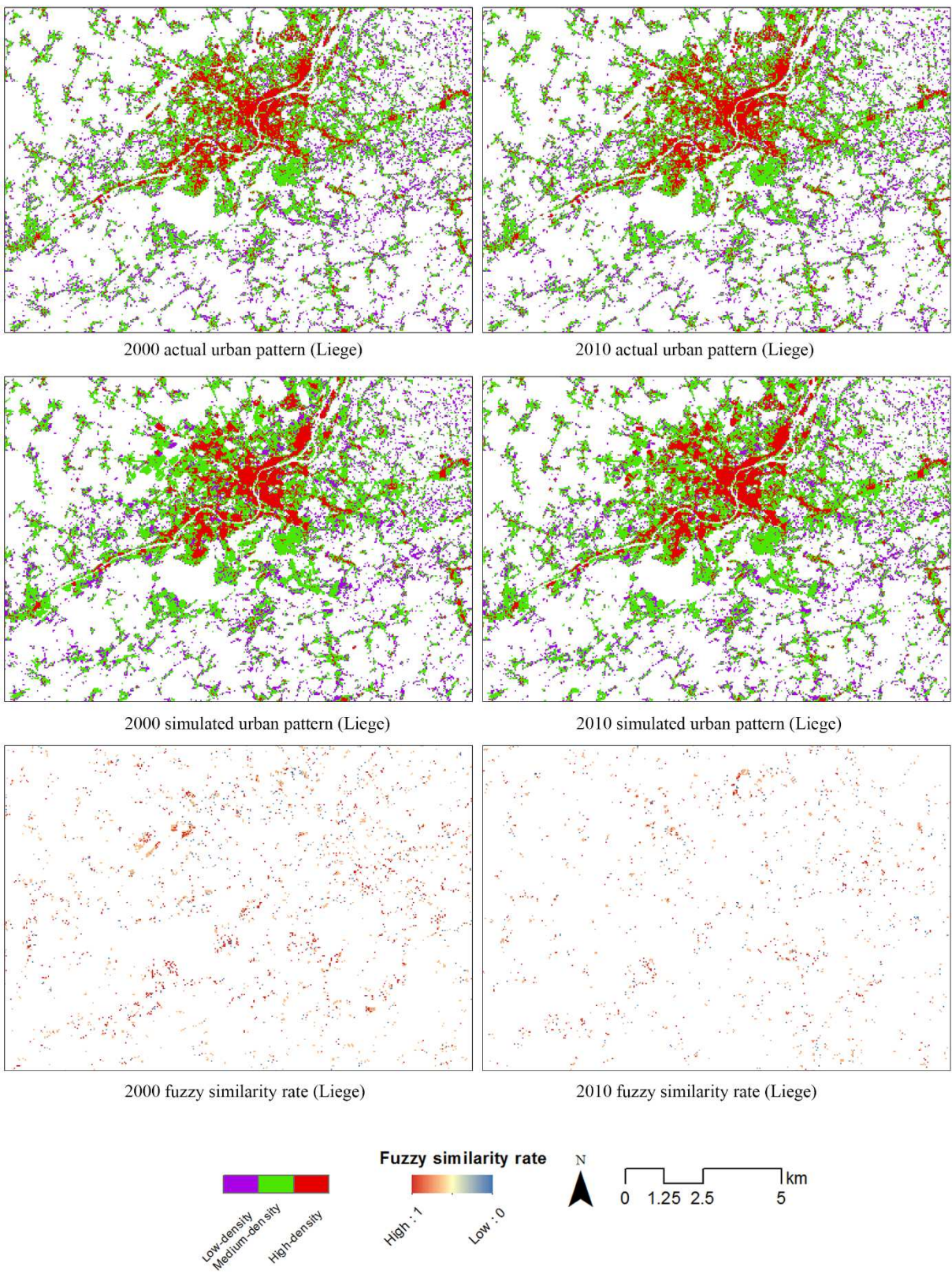
2000 actual urban pattern (Liege)

2010 actual urban pattern (Liege)

2000 simulated urban pattern (Liege)

2010 simulated urban pattern (Liege)

2000 fuzzy similarity rate (Liege)

2010 fuzzy similarity rate (Liege)

Fuzzy similarity rate

Low-density   Medium-density   High-density

High : 1   Low : 0

N

0   1.25 2.5   5   km

385
386   **Figure 7:** The actual and simulated 2000 and 2010 built-up patterns for Liege metropolitan.

387 The simulation of the 2000 and 2010 built-up patterns in the major metropolitan area (Liege),

388 as an example, are shown in Figure 7.

5. Conclusion

390 One of the central limitations of most existing built-up/urban expansion models is that

391 urbanization is considered as a binary process (built-up/non built-up). This research has

392 demonstrated that the built-up development process is heterogeneous, with links between density

393 and the impact of different built-up development causative factors. We propose an integrated

394 multinomial logistic regression (MLR) and cellular automata (CA) model to examine the built-up

395 development trends in Wallonia (Belgium). The built-up development considers both expansion

396 and densification. Considering the densification is an essential component of sprawl-fighting

397 land-use policies. In this study, built-up densities (non built-up, low-density, medium-density

398 and high-density) for 1990, 2000 and 2010 and geophysical and socioeconomic data that are

399 referred to as causative factors were gathered and processed.

400 The MLR allows to automate the calibration of the causative factors whereas the CA model is

401 used to simulate the neighborhood interactions. A multi-objective/genetic algorithm is employed

402 to calibrate neighborhood interactions parameters. The calibration is done for built-up transitions

403 between 1990 and 2000. The calibration results are then used to validate the model by simulating

404 the 2010 built-up pattern and compare it with the actual 2010 built-up. The model evaluates the

405 MLR outcomes using relative operating characteristic and validates the simulated built-up

406 patterns by means of fuzzy set theory. The model reveals a good overall accuracy. However,

407 calibration and validation processes provide information on the uncertainties in the model

408 outcomes over time. In later work we intend to pursue the analysis further by quantifying and

409   modelling uncertainty in the future built-up simulations. Therefore, our model can effectively

410   develop future built-up scenarios considering the uncertainty.

411   The findings drawn from this study suggest that all selected factors have impacts on the

412   expansion in Wallonia, but their relative importance varied with density. However, zoning status,

413   slope, and distance to local roads are the most important determinants of the expansion process.

414   In regards to the densification process, it is mainly driven by zoning, slope, distance to different

415   roads and richness index. The magnitude of the effect of land-use policies (zoning) decline along

416   with the densification process. The neighborhood effect weights imply that the densification

417   occurs in already dense areas whereas low-density and medium-density areas tend to retain their

418   densities over time. Public authorities clearly should play a role in the development of a more

419   balanced densification policy, considering the densification of very accessible (transport,

420   services, etc) low/medium density nodes besides a further densification of already dense areas.

421   This is not contradictory with a concentration spatial policy provided that low/medium density

422   nodes where densification occurs are well connected to city centers (as for instance promoted

423   through transit-oriented development).

424   This study identifies the most notable built-up development factors at different densities. Our

425   analysis does not consider building use or height. There are several missing of buildings uses and

426   heights within the cadastral data. Consequently, population and employment density indices

427   cannot be considered here. However, this study prompts a series of further research questions

428   regarding the relation between built-up density and land-use policy, spatial, geophysical and

429   socioeconomic factors. Hopefully this study should provide a useful context for policy makers

430   and the ongoing research.

431

References

Aburas, M.M., Ho, Y.M., Ramli, M.F., Ash'aari, Z.H., 2016. The simulation and prediction of spatio-temporal urban growth trends using cellular automata models: A review. Int. J. Appl. Earth Obs. Geoinformation 52, 380–389. doi:10.1016/j.jag.2016.07.007

Achmad, A., Hasyim, S., Dahlan, B., Aulia, D.N., 2015. Modeling of urban growth in tsunami-prone city using logistic regression: Analysis of Banda Aceh, Indonesia. Appl. Geogr. 62, 237–246. doi:10.1016/j.apgeog.2015.05.001

Ahmed, B., Ahmed, R., Zhu, X., 2013. Evaluation of Model Validation Techniques in Land Cover Dynamics. ISPRS Int. J. Geo-Inf. 2, 577–597. doi:10.3390/ijgi2030577

Al-Ahmadi, K., See, L., Heppenstall, A., Hogg, J., 2009. Calibration of a fuzzy cellular automata model of urban dynamics in Saudi Arabia. Ecol. Complex. 6, 80–101. doi:10.1016/j.ecocom.2008.09.004

Arlinghaus, S.L., Kerski, J.J., 2013. Spatial Mathematics: Theory and Practice through Mapping. CRC Press.

Beckers, A., Dewals, B., Erpicum, S., Dujardin, S., Detrembleur, S., Teller, J., Pirotton, M., Archambeau, P., 2013. Contribution of land use changes to future flood damage along the river Meuse in the Walloon region. Nat Hazards Earth Syst Sci 13, 2301–2318. doi:10.5194/nhess-13-2301-2013

Belgian Federal Government, 2013. Statistics Belgium [WWW Document]. Stat. Belg. URL http://statbel.fgov.be/fr/statistiques/chiffres/ (accessed 4.29.14).

Berberoğlu, S., Akın, A., Clarke, K.C., 2016. Cellular automata modeling approaches to forecast urban growth for adana, Turkey: A comparative approach. Landsc. Urban Plan. 153, 11–27. doi:10.1016/j.landurbplan.2016.04.017

Cammerer, H., Thieken, A.H., Verburg, P.H., 2013. Spatio-temporal dynamics in the flood exposure due to land use changes in the Alpine Lech Valley in Tyrol (Austria). Nat. Hazards 68, 1243–1270. doi:10.1007/s11069-012-0280-8

Chen, Y., Li, X., Liu, X., Ai, B., 2014. Modeling urban land-use dynamics in a fast developing city using the modified logistic cellular automaton with a patch-based simulation strategy. Int. J. Geogr. Inf. Sci. 28, 234–255. doi:10.1080/13658816.2013.831868

Clarke, K.C., Gaydos, L.J., 1998. Loose-coupling a cellular automaton model and GIS: long-term urban growth prediction for San Francisco and Washington/Baltimore. Int. J. Geogr. Inf. Sci. 12, 699–714. doi:10.1080/136588198241617

Clarke, K.C., Hoppen, S., Gaydos, L., 1997. A Self-Modifying Cellular Automaton Model of Historical Urbanization in the San Francisco Bay Area. Environ. Plan. B Plan. Des. 24, 247–261. doi:10.1068/b240247

Crols, T., White, R., Uljee, I., Engelen, G., Poelmans, L., Canters, F., 2015. A travel time-based variable grid approach for an activity-based cellular automata model. Int. J. Geogr. Inf. Sci. 29, 1757–1781. doi:10.1080/13658816.2015.1047838

Deb, K., 2001. Multi-Objective Optimization Using Evolutionary Algorithms. John Wiley & Sons.

Dieleman, F., Wegener, M., 2004. Compact City and Urban Sprawl. Built Environ. 1978- 30, 308–323.

Dubovyk, O., Sliuzas, R., Flacke, J., 2011. Spatio-temporal modelling of informal settlement development in Sancaktepe district, Istanbul, Turkey. ISPRS J. Photogramm. Remote Sens., Quality, Scale and Analysis Aspects of Urban City Models 66, 235–246. doi:10.1016/j.isprsjprs.2010.10.002

Feng, Y., Liu, Y., Tong, X., Liu, M., Deng, S., 2011. Modeling dynamic urban growth using cellular automata and particle swarm optimization rules. Landsc. Urban Plan. 102, 188–196. doi:10.1016/j.landurbplan.2011.04.004

García, A.M., Santé, I., Boullón, M., Crecente, R., 2013. Calibration of an urban cellular automaton model by using statistical techniques and a genetic algorithm. Application to a small urban settlement of NW Spain. Int. J. Geogr. Inf. Sci. 27, 1593–1611. doi:10.1080/13658816.2012.762454

García, A.M., Santé, I., Boullón, M., Crecente, R., 2012. A comparative analysis of cellular automata models for simulation of small urban areas in Galicia, NW Spain. Comput. Environ. Urban Syst. 36, 291–301. doi:10.1016/j.compenvurbsys.2012.01.001

Hagen, A., 2003. Fuzzy set approach to assessing similarity of categorical maps. Int. J. Geogr. Inf. Sci. 17, 235–249. doi:10.1080/13658810210157822

Han, J., Hayashi, Y., Cao, X., Imura, H., 2009. Application of an integrated system dynamics and cellular automata model for urban growth assessment: A case study of Shanghai, China. Landsc. Urban Plan. 91, 133–141. doi:10.1016/j.landurbplan.2008.12.002

Han, Y., Jia, H., 2016. Simulating the spatial dynamics of urban growth with an integrated modeling approach: A case study of Foshan, China. Ecol. Model. doi:10.1016/j.ecolmodel.2016.04.005

Hansheng, L., Lishan, K., 1999. Balance between exploration and exploitation in genetic search. Wuhan Univ. J. Nat. Sci. 4, 28–32. doi:10.1007/BF02827615

Holland, J.H., 1975. Adaptation in natural and artificial systems. U Michigan Press, Oxford, England.

Hu, Z., Lo, C.P., 2007. Modeling urban growth in Atlanta using logistic regression. Comput. Environ. Urban Syst. 31, 667–688. doi:10.1016/j.compenvurbsys.2006.11.001

Jiang, F., Liu, S., Yuan, H., Zhang, Q., 2007. Measuring urban sprawl in Beijing with geo-spatial indices. J. Geogr. Sci. 17, 469–478. doi:10.1007/s11442-007-0469-z

Jr, D.W.H., Lemeshow, S., 2004. Applied Logistic Regression. John Wiley & Sons.

Kim, J.-H., 2003. Assessing practical significance of the proportional odds assumption. Stat. Probab. Lett. 65, 233–239. doi:10.1016/j.spl.2003.07.017

Kumar, A., Pandey, A.C., Jeyaseelan, A.T., 2012. Built-up and vegetation extraction and density mapping using WorldView-II. Geocarto Int. 27, 557–568. doi:10.1080/10106049.2012.657695

Li, X., Zhou, W., Ouyang, Z., 2013. Forty years of urban expansion in Beijing: What is the relative importance of physical, socio-economic, and neighborhood factors? Appl. Geogr. 38, 1–10. doi:10.1016/j.apgeog.2012.11.004

Liao, J., Tang, L., Shao, G., Qiu, Q., Wang, C., Zheng, S., Su, X., 2014. A neighbor decay cellular automata approach for simulating urban expansion based on particle swarm intelligence. Int. J. Geogr. Inf. Sci. 28, 720–738. doi:10.1080/13658816.2013.869820

Liu, X., Ma, L., Li, X., Ai, B., Li, S., He, Z., 2014. Simulating urban growth by integrating landscape expansion index (LEI) and cellular automata. Int. J. Geogr. Inf. Sci. 28, 148–163. doi:10.1080/13658816.2013.831097

Loibl, W., Toetzer, T., 2003. Modeling growth and densification processes in suburban regions—simulation of landscape transition with spatial agents. Environ. Model. Softw., Applying Computer Research to Environmental Problems 18, 553–563. doi:10.1016/S1364-8152(03)00030-6

Loibl, W., Tötzer, T., Köstl, M., Steinnocher, K., 2007. Simulation of Polycentric Urban Growth Dynamics Through Agents, in: Koomen, E., Stillwell, J., Bakema, A., Scholten, H.J. (Eds.), Modelling Land-Use Change, The GeoJournal Library. Springer Netherlands, pp. 219–236. doi:10.1007/978-1-4020-5648-2_13

Montgomery, D.C., Runger, G.C., 2003. Applied Statistics and Probability for Engineers, Fourth. ed. John Wiley & Sons, New York.

Munshi, T., Zuidgeest, M., Brussel, M., van Maarseveen, M., 2014. Logistic regression and cellular automata-based modelling of retail, commercial and residential development in the city of Ahmedabad, India. Cities 39, 68–86. doi:10.1016/j.cities.2014.02.007

Mustafa, A., Cools, M., Saadi, I., Teller, J., 2015. Urban Development as a Continuum: A Multinomial Logistic Regression Approach, in: Gervasi, O., Murgante, B., Misra, S., Gavrilova, M.L., Rocha, A.M.A.C., Torre, C., Taniar, D., Apduhan, B.O. (Eds.), Computational Science and Its Applications -- ICCSA 2015, Lecture Notes in Computer Science. Springer International Publishing, pp. 729–744.

Mustafa, A., Saadi, I., Cools, M., Teller, J., 2014. Measuring the Effect of Stochastic Perturbation Component in Cellular Automata Urban Growth Model. Procedia Environ. Sci., 12th International Conference on Design and Decision Support Systems in Architecture and Urban Planning, DDSS 2014 22, 156–168. doi:10.1016/j.proenv.2014.11.016

Nabielek, K., 2012. The Compact City: Planning strategies, recent developments and future prospects in the Netherlands - PBL Netherlands Environmental Assessment Agency, in: Proceedings of the AESOP 26th Annual Congress. Presented at the AESOP 26th Annual Congress, Ankara.

Omrani, H., Abdallah, F., Charif, O., Longford, N.T., 2015. Multi-label class assignment in land-use modelling. Int. J. Geogr. Inf. Sci. 29, 1023–1041. doi:10.1080/13658816.2015.1008004

Overmars, K.P., de Koning, G.H.J., Veldkamp, A., 2003. Spatial autocorrelation in multi-scale land use models. Ecol. Model. 164, 257–270. doi:10.1016/S0304-3800(03)00070-X

Poelmans, L., Van Rompaey, A., 2010. Complexity and performance of urban expansion models. Comput. Environ. Urban Syst. 34, 17–27. doi:10.1016/j.compenvurbsys.2009.06.001

Poelmans, L., Van Rompaey, A., 2009. Detecting and modelling spatial patterns of urban sprawl in highly fragmented areas: A case study in the Flanders–Brussels region. Landsc. Urban Plan. 93, 10–19. doi:10.1016/j.landurbplan.2009.05.018

Puertas, O.L., Henríquez, C., Meza, F.J., 2014. Assessing spatial dynamics of urban growth using an integrated land use model. Application in Santiago Metropolitan Area, 2010–2045. Land Use Policy 38, 415–425. doi:10.1016/j.landusepol.2013.11.024

Rienow, A., Goetzke, R., 2015. Supporting SLEUTH – Enhancing a cellular automaton with support vector machines for urban growth modeling. Comput. Environ. Urban Syst. 49, 66–81. doi:10.1016/j.compenvurbsys.2014.05.001

Robinson, D.T., Murray-Rust, D., Rieser, V., Milicic, V., Rounsevell, M., 2012. Modelling the impacts of land system dynamics on human well-being: Using an agent-based approach to cope with data limitations in Koper, Slovenia. Comput. Environ. Urban Syst., Special Issue: Geoinformatics 2010 36, 164–176. doi:10.1016/j.compenvurbsys.2011.10.002

Roy Chowdhury, P.K., Maithani, S., 2014. Modelling urban growth in the Indo-Gangetic plain using nighttime OLS data and cellular automata. Int. J. Appl. Earth Obs. Geoinformation 33, 155–165. doi:10.1016/j.jag.2014.04.009

Santé, I., García, A.M., Miranda, D., Crecente, R., 2010. Cellular automata models for the simulation of real-world urban processes: A review and analysis. Landsc. Urban Plan. 96, 108–122. doi:10.1016/j.landurbplan.2010.03.001

Shan, J., Alkheder, S., Wang, J., 2008. Genetic Algorithms for the Calibration of Cellular Automata Urban Growth Modeling. Photogramm. Eng. Remote Sens. 74, 1267–1277. doi:10.14358/PERS.74.10.1267

Sunde, M.G., He, H.S., Zhou, B., Hubbart, J.A., Spicci, A., 2014. Imperviousness Change Analysis Tool (I-CAT) for simulating pixel-level urban growth. Landsc. Urban Plan. 124, 104–108. doi:10.1016/j.landurbplan.2014.01.007

Tachieva, G., 2010. Sprawl Repair Manual, 2 edition. ed. Island Press, Washington.

Tannier, C., Thomas, I., 2013. Defining and characterizing urban boundaries: A fractal analysis of theoretical cities and Belgian cities. Comput. Environ. Urban Syst. 41, 234–248. doi:10.1016/j.compenvurbsys.2013.07.003

Thomas, I., Frankhauser, P., Biernacki, C., 2008. The morphology of built-up landscapes in Wallonia (Belgium): A classification using fractal indices. Landsc. Urban Plan. 84, 99–115. doi:10.1016/j.landurbplan.2007.07.002

Tian, G., Ma, B., Xu, X., Liu, Xiaoping, Xu, L., Liu, Xiaojuan, Xiao, L., Kong, L., 2016. Simulation of urban expansion and encroachment using cellular automata and multi-agent system model—A case study of Tianjin metropolitan region, China. Ecol. Indic., Navigating Urban Complexity: Advancing Understanding of Urban Social – Ecological Systems for Transformation and Resilience 70, 439–450. doi:10.1016/j.ecolind.2016.06.021

van Vliet, J., Bregt, A.K., Brown, D.G., van Delden, H., Heckbert, S., Verburg, P.H., 2016. A review of current calibration and validation practices in land-change modeling. Environ. Model. Softw. 82, 174–182. doi:10.1016/j.envsoft.2016.04.017

Verburg, P.H., van Eck, J.R.R., de Nijs, T.C.M., Dijst, M.J., Schot, P., 2004. Determinants of Land-Use Change Patterns in the Netherlands. Environ. Plan. B Plan. Des. 31, 125–150. doi:10.1068/b307

Vermeiren, K., Van Rompaey, A., Loopmans, M., Serwajja, E., Mukwaya, P., 2012. Urban growth of Kampala, Uganda: Pattern analysis and scenario development. Landsc. Urban Plan. 106, 199–206. doi:10.1016/j.landurbplan.2012.03.006

Wang, H., He, S., Liu, X., Dai, L., Pan, P., Hong, S., Zhang, W., 2013. Simulating urban expansion using a cloud-based cellular automata model: A case study of Jiangxia, Wuhan, China. Landsc. Urban Plan. 110, 99–112. doi:10.1016/j.landurbplan.2012.10.016

Ward, D.P., Murray, A.T., Phinn, S.R., 2000. A stochastically constrained cellular model of urban growth. Comput. Environ. Urban Syst. 24, 539–558. doi:10.1016/S0198-9715(00)00008-9

White, R., Engelen, G., 2000. High-resolution integrated modelling of the spatial dynamics of urban and regional systems. Comput. Environ. Urban Syst. 24, 383–400. doi:10.1016/S0198-9715(00)00012-0

White, R., Engelen, G., 1997. Cellular Automata as the Basis of Integrated Dynamic Regional Modelling. Environ. Plan. B Plan. Des. 24, 235–246. doi:10.1068/b240235

White, R., Engelen, G., Uljee, I., 2015. The Cellular Automaton Eats the Regions: Unified Modeling of Activities and Land Use in a Variable Grid Cellular Automaton, in: Modeling Cities and Regions As Complex Systems: From Theory to Planning Applications. The MIT Press, Cambridge , Massachusetts.

White, R., Uljee, I., Engelen, G., 2012. Integrated modelling of population, employment and land-use change with a multiple activity-based variable grid cellular automaton. Int. J. Geogr. Inf. Sci. 26, 1251–1280. doi:10.1080/13658816.2011.635146

Wu, F., 2002. Calibration of stochastic cellular automata: the application to rural-urban land conversions. Int. J. Geogr. Inf. Sci. 16, 795–818. doi:10.1080/13658810210157769

Xian, G., Crane, M., 2005. Assessments of urban growth in the Tampa Bay watershed using remote sensing data. Remote Sens. Environ. 97, 203–215. doi:10.1016/j.rse.2005.04.017

Yang, X., 2010. Integration of Remote Sensing with GIS for Urban Growth Characterization, in: Jiang, B., Yao, X. (Eds.), Geospatial Analysis and Modelling of Urban Structure and Dynamics, GeoJournal Library. Springer Netherlands, pp. 223–250. doi:10.1007/978-90-481-8572-6_12

Yijie, S., Gongzhang, S., 2008. Improved NSGA-II Multi-objective Genetic Algorithm Based on Hybridization-encouraged Mechanism. Chin. J. Aeronaut. 21, 540–549. doi:10.1016/S1000-9361(08)60172-7

Zhang, Q., Ban, Y., Liu, J., Hu, Y., 2011. Simulation and analysis of urban growth scenarios for the Greater Shanghai Area, China. Comput. Environ. Urban Syst., Geospatial Analysis and Modeling 35, 126–139. doi:10.1016/j.compenvurbsys.2010.12.002